(4) W. Klöpffer, "Organic Molecular Photophysics", Vol. 1, J. B. Birks, Ed., Wiley, New York, N.Y., 1973, Chapter 7.
(5) S. S. Yanari, F. A. Bovey, and R. Lumry, *Nature (London)*, **200**, 242 (1963).
(6) U. Wang and H. Morawetz, *Makromol. Chem., Suppl.*, **1**, 283 (1975).
(7) G. E. Johnson, *J. Chem. Phys.*, **62**, 4697 (1975).
(8) T. Ishii, T. Handa, and S. Matsungaga, *Makromol. Chem.*, **177**, 283 (1976).
(9) T. Ishii, T. Handa, and S. Matsunaga, *Makromol. Chem.*, **178**, 2351 (1977).
(10) W. H. Stockmayer and K. Matsuo, *Macromolecules*, **5**, 766 (1972).
(11) A. Allerhand and R. K. Heilstone, *J. Chem. Phys.*, **56**, 3718 (1972).
(12) A. T. Bullock, G. G. Cameron, and P. M. Smith, *J. Phys. Chem.*, **77**, 1635 (1973).
(13) H. Nomura and Y. Miyahara, *Polym. J.*, **8**, 30 (1976).
(14) D. R. Bauer, J. I. Brauman, and R. Pecora, *Macromolecules*, **8**, 443 (1975).
(15) Ye. V. Anufrieva, Yu. Ya. Gotlib, and M. G. Krakovyak, *Vyskomol. Soedin., Ser. A*, **15**, 2538 (1973).
(16) J. A. Riddick and W. B. Punger, "Organic Solvents", Wiley, New York, N.Y., 1970.
(17) C. A. Parker, *Anal. Chem.*, **34**, 502 (1962).
(18) T. Ishii, H. Matsushita, and T. Handa, *Kobunshi Ronbunshu*, **32**, 211 (1975).
(19) J. B. Birks, "Photopysics of Aromatic Molecules", Wiley-Interscience, New York, N.Y., 1970, Chapters 7 and 11.
(20) F. Heisel and H. Laustriat, *J. Chim. Phys. Phys.-Chim. Biol.*, **66**, 1895 (1969).
(21) J. B. Birks, D. J. Dyson, and I. H. Munro, *Proc. R. Soc. London, Ser. A*, **275**, 575 (1963).
(22) J. B. Birks, D. J. Dyson, and T. A. King, *Proc. R. Soc. London, Ser. A*, **277**, 270 (1964).
(23) W. Klöpffer and W. Liptay, *Z. Naturforsch., A* **25**, 1091 (1970).
(24) W. Klöpffer, *Ber. Bunsenges. Phys. Chem.*, **74**, 693 (1970).
(25) E. A. Chandross and C. J. Dempster, *J. Am. Chem. Soc.*, **92**, 3586 (1970).
(26) L. A. Harrah, *J. Chem. Phys.*, **56**, 385 (1972).
(27) C. W. Frank and L. A. Harrah, *J. Chem. Phys.*, **61**, 1526 (1974).
(28) J. B. Birks and J. C. Conte, *Proc. R. Soc. London, Ser. A*, **303**, 85 (1974).
(29) J. N. Movaghar, J. B. Birks, and K. R. Nagvi, *Proc. Phys. Soc., London*, **91**, 449 (1967).
(30) C. David, N. P. Lavoreille, and G. Geuskens, *Eur. Polym. J.*, **10**, 617 (1974).
(31) G. Natta, *Makromol. Chem.*, **35**, 94 (1960).
(32) G. Fourche and B. Lemaire, *Polym. J.*, **4**, 476 (1973).
(33) C. W. Frank, *J. Chem. Phys.*, **61**, 2015 (1974).
(34) W. Klöpffer, *J. Chem. Phys.*, **50**, 2337 (1969).
(35) J. Yugerabide, *J. Chem. Phys.*, **49**, 1026 (1968).
(36) C. Lewis and W. R. Ware, *J. Chem. Soc., Faraday Trans. 2*, **72**, 1851 (1976).
(37) A. H. Alwattar, M. D. Lumb, and J. B. Birks, "Organic Molecular Phtophysics", Vol. 1, J. B. Birks, Ed., Wiley, New York, N.Y., 1973, Chapter 8.
(38) E. Leroy, C. F. Lapp, and G. Laustriat, *Biopolymers*, **13**, 507 (1974).
(39) A. Ueno, T. Osa, and F. Toda, *Macromolecules*, **10**, 130 (1977).
(40) W. R. Ware, *J. Phys. Chem.*, **66**, 455 (1962).
(41) P. K. Ludig and C. D. Amata, *J. Chem. Phys.*, **49**, 333 (1968).

Size and Density of Fibrin Fibers from Turbidity[1]

Marcus E. Carr, Jr., and Jan Hermans*

Department of Biochemistry, School of Medicine, University of North Carolina, Chapel Hill, North Carolina 27514. *Received September 1, 1977*

ABSTRACT: In agreement with earlier observations that the angular dependence of light scattering by fibrin gels obeys the theory for light scattering by very long and thin rigid rodlike particles (intensity proportional to the square of half the scattering angle), we find that the turbidity, τ, of the less opaque gels varies as the inverse third power of the wavelength, λ. Mass–length ratios of the fibers calculated from these two measurements closely agree. For fibrin gels containing fibers with a very high mass–length ratio (of which we had not been able to obtain interpretable scattering data), the turbidity is found not quite to vary as $1/\lambda^3$. For these opaque gels, the fiber diameter is no longer negligible with respect to the wavelength. It is shown how the radius of gyration of the fiber cross section (and therefore the radius of cylindrical fibers) can be obtained from the ratio of slope and intercept of a plot of $1/\tau\lambda^3$ vs. $1/\lambda^2$. The square of the radius of the fibers is found to be proportional to the mass–length ratio. The density of the fibers is calculated to be 0.28. This corresponds to a ratio of fiber volume to volume of protein contained in the fiber of 5.0.

When the plasma protein fibrinogen is acted upon by the enzyme thrombin, it is irreversibly converted to fibrin monomer. Fibrin monomers rapidly form a network of fibrin fibers which, in vitro, turn the solution into a gel, and, in vivo, form a hemostatic plug at a lesion of the circulatory system. (For successive reviews see ref 2–4.)

The gelation of fibrin can be followed by a variety of methods. The most direct of these is the detection or measurement of the rigidity of the gel. The detection of rigidity is often qualitative since its measurement requires the use of equipment that is not widely available. Hence, less direct methods are used more commonly. Of these methods, one is to determine the amount of fibrin fiber as the fraction of insoluble material (clottability). Another is to follow the increase in turbidity or light scattering due to the formation of the fibers. The work reported below was begun with the intention of examining the physical basis of this last method.

All our experiments were done with purified fibrinogen of high clottability and gelation was obtained by addition of thrombin. It is well known that the properties of fibrin gels vary markedly as the solutions in which they are formed are changed, for example, as to ionic strength or pH.[5–8] In particular, the diameter of the fibers is variable; the mass–length ratio of the fibers varies by a factor of at least 100, depending on the solvent.[9] We have used this fact in order to prepare fibrin gels with fibers of different mass–length ratio. Of these gels, we measured the turbidity and the light scattering.

Electron micrographs of fibrin show that the fibers are not bent significantly over distances of several microns.[10–14] One expects that the light scattering by such fibers is the same as that predicted theoretically for very long and thin rodlike particles. We have recently confirmed that this is the case for relatively transparent fibrin gels.[9] The scattering of the more opaque gels (which are typical of gels formed under physiological conditions) is hopelessly affected by their high turbidity, at least when measured in our instrument. Since the turbidity is simply the scattering integrated over all directions, it should be possible to test also if the turbidities of the opaque gels are in agreement with the theory for scattering by very long rods.

As a result of this work, we conclude that one can use the turbidity of a fibrin gel in order to calculate a reliable average mass–length ratio of the fibers in the gel. Furthermore, for very massive fibers, the wavelength dependence of the turbidity can be used to calculate also the average radius of the fibers.

0024-9297/78/2211-0046$01.00/0

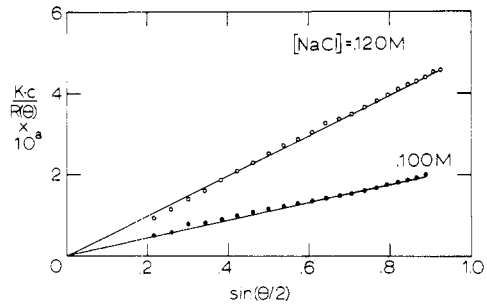

Figure 1. Angular dependence of light scattering by two fibrin gels. The inverse of the Rayleigh ratio is plotted as a function of the sine of half the scattering angle. Fibrin concentration 1.0 mg/mL, thrombin concentration 1.25 units/mL. The gels contain different concentrations of NaCl.

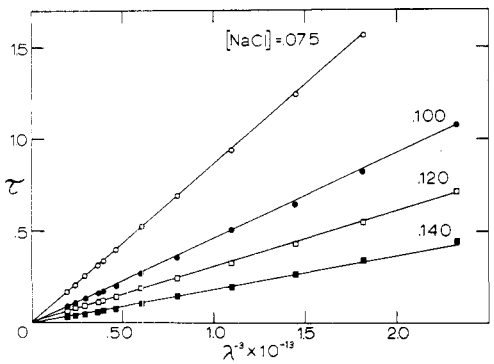

Figure 2. Wavelength dependence of the turbidity of four fibrin gels. These gels were prepared in the same way as were those of Figure 1.

I. Experimental Section

A. Materials. Human fibrinogen (Grade L, A.B. Kabi, Stockholm, Sweden) was dissolved in 0.3 M NaCl at 25 °C. The solution was cleared by centrifugation at 30 000 g for 20 min. In order to remove any free calcium it was dialyzed against 0.3 M NaCl for 18 h. The solution was then divided into lots and frozen at −70 °C for storage. Clottability was greater than 95%. Fibrinogen concentration was determined from absorbance at 280 nm using a specific extinction coefficient of 1.6 mL/(mg cm).

Thrombin solutions were prepared by dissolving Parke-Davis bovine thrombin in water to reach a concentration of 200 NIH units/mL. Free calcium was removed by dialysis. The thrombin was stored in small aliquots at −70 °C.

B. Methods. Turbidity measurements were made using a Zeiss PMQII spectrophotometer. The turbidity is, of course, equal to the ratio of optical density to sample thickness multiplied by ln 10 (=2.303). In principle, turbidity measurements are always in error because *some* scattered light is collected by the detector. The error can be minimized by using a primary beam with a small diameter. We have installed two diaphragms in the spectrophotometer, one in front of the cell, in order to create a narrow primary beam, and the other in front of the detector of a size to just let pass the entire primary beam. Since we measure essentially the same turbidities with or without the diaphragms, we conclude that the error due to the finite cross section of the beam is not a serious one for this instrument.

The apparatus used for light-scattering measurements has been described previously.[9] Benzene was used as a standard scatterer. The Rayleigh ratio for benzene at 90° was taken to be 6.6×10^{-6} cm^{-1} (for an unpolarized incident beam[9]).

Measurements of turbidity and of 90° scattering were made using 1- and 2-cm rectangular cells with clear windows on four sides. The angular dependence of the scattering was measured using 29-mm cylindrical cells. All cells were hand washed in detergent, soaked overnight in concentrated nitric acid, rinsed in deionized redistilled water, and dried in an oven at 125 °C prior to use.

The clotting solutions were formed by rapid mixing of thrombin and fibrinogen solutions. The final solutions were buffered at pH 7.4 with 0.05 M tris and contained 5 mM $CaCl_2$. The solutions also contained NaCl. The concentrations of NaCl and thrombin were varied in order to control the fiber thickness.[5] All solutions used in light-scattering experiments, with the exception of the fibrinogen stock solution, were filtered through pre-soaked filters (GS 0.22 μm; Millipore Filter Corp., Bedford, Mass.).

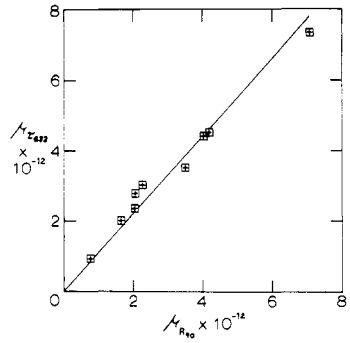

Figure 3. Correlation of the mass–length ratios (in dalton/cm) calculated from the turbidity and from the 90° scattering intensity, both at 633 nm, of a number of fibrin gels formed under different conditions.

The measurements were made with respect to blanks which contained all components of the clotting solutions except fibrinogen. In all cases the kinetics of formation of the fibers were followed by measurement of either the scattering or the turbidity at 633 nm. The measurements reported below were performed after no measurable increase of turbidity or scattering had been noted for 20 min.

II. Results

A. Mass–Length Ratio. We wished to establish that the mass–length ratio of fibrin fibers can be obtained from turbidity measurements. We had already shown[9] that the angular dependence of scattering by fibrin gels containing fibers of low mass–length ratio obeys the theory for scattering by very long and thin rodlike particles. The angular dependence of the scattering by two gels, plotted in such a way as to give straight lines passing through the origin if this theory applies, is shown in Figure 1 (cf. eq 3 and ref 9). The same theory can be extended to the turbidity of similar rodlike particles (see below). The turbidity is predicted to be proportional to the inverse third power of the wavelength. Turbidities measured in the range from 350 to 650 nm are plotted in Figure 2. It is obvious that the predicted proportionality holds rather well.

Theory also requires that the two proportionalities, i.e., the slopes of the plots of Figures 1 and 2, be related. Since we found some variability of the turbidity and scattering of different gels prepared in the same manner, we measured the turbidity and the 90° scattering intensity of the same gels, both at 633 nm, and calculated the mass–length ratios from each of these measurements, using the theoretical expressions for very long and thin rodlike particles, eq 3 and 5.

The results of this comparison are shown in Figure 3. The mass–length ratios calculated from the turbidities tend to be higher than those calculated from the light scattering by about 10%. This systematic difference may indicate a corresponding error in the value of the Rayleigh ratio of the standard (benzene) used in our calculations.

The mass–length ratio calculated from the turbidity is somewhat lower than the value that we had obtained from the gel's permeability.[9] The respective values are 17.4×10^{12} and 26×10^{12} dalton/cm (for a gel containing 1.0 mg/mL fibrin and 0.05 M NaCl).

B. Fiber Radius. When we changed the conditions of gelation in order to favor the formation of very turbid gels, we found that the proportionality of the turbidity, τ, to the inverse third power of the wavelength, λ, did not continue to hold. When the method for obtaining turbid gels consisted of lowering the thrombin concentration and/or raising the fi-

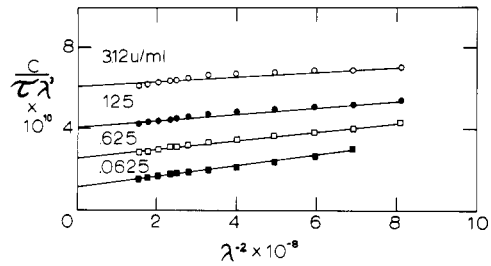

Figure 4. Wavelength dependence of the turbidity of several fibrin gels with a high mass–length ratio. The data have been fitted with straight lines. The intercept of these lines is proportional to the reciprocal of the mass–length ratio, and the ratio of slope and intercept is proportional to the square of the radius of the fibers. The solution contains 1 mg/mL fibrin and 0.1 M NaCl, pH 7.4. The thrombin concentration is indicated by each curve.

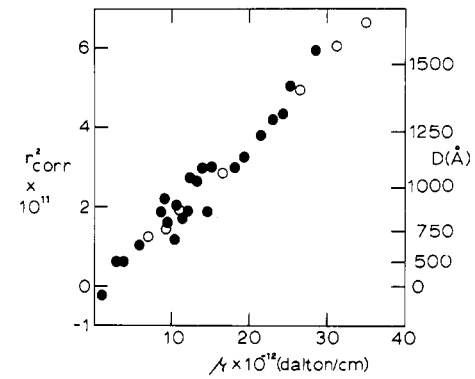

Figure 5. Correlation of the square of the fiber radius with the fiber mass–length ratio. The open symbols indicate a series of samples prepared with different thrombin concentrations but of otherwise identical composition (1.0 mg/mL fibrinogen, 0.05 M tris buffer, pH 7.4, 0.05 M NaCl). The right-hand scale indicates the fiber diameter.

brinogen concentration, we found that the plots of τ as a function of λ^{-3} were curved but did extrapolate to the origin. Presumably, the initial slope of these plots may be used to calculate the mass–length ratio of the fibers. However, we prefer to plot these data as $c/\tau\lambda^3$ (where c is the fibrin concentration) as a function of λ^{-2}. One may then use the intercept of such a plot to calculate the mass–length ratio of the fibers and its initial slope to calculate the fiber radius. The results for several fibrin gels plotted in this manner are shown in Figure 4.

If such plots are made using data for gels containing fibers of a low mass–length ratio whose radius is insignificant, one obtains curves which have a slight negative slope rather than a slope of zero. This is not unexpected, since the wavelength dependence (dispersion) of a factor $n(dn/dc)^2$ which occurs in the theoretical expression for the turbidity (cf. eq 4 and 5) has been neglected. A correction for this dispersion can be applied very simply by adding a constant term to each value of r^2 calculated from slope and intercept of a plot of $c/\tau\lambda^3$ vs. λ^{-2}. From turbidities of samples containing fibers with a low mass–length ratio, we estimate that this correction is ca. 1.0×10^{-11}; from values of n and dn/dc at several wavelengths[9,15] one obtains a similar estimate.

Figure 5 shows results for several series of gels, in the form of a plot of the (corrected) square of the fiber radius as a function of the mass–length ratio.

Finally, it should be mentioned that when the method for obtaining turbid gels consisted of lowering the ionic strength and raising the fibrin concentration, we eventually obtained results that did *not* fit the above description. At the lowest salt concentration (0.06 M NaCl) and at a fibrin concentration of 2.0 mg/mL, the plots of τ as a function of λ^{-3} did not extrapolate to the origin. Since fibrinogen is known to precipitate from solution at low ionic strength, we suggest that in this case some fraction of the protein was present in the form of a precipitate of fibrinogen or fibrin rather than in the form of fibrin fibers.

III. Discussion

The presence of fibers of different thickness in fibrin gels with different turbidity was first proposed by Ferry[2,5] and has since been confirmed with electron microscopy.[10–14] Ferry originally distinguished between two extreme categories, "coarse" and "fine" gels, but it is now clear that fibrin fibers can vary in size from a minimum size protofibril, with two molecules in the fiber cross section and a mass–length ratio of 1.5×10^{11} dalton/cm, to very massive fibers for which these numbers are many hundred times greater.[9] The results of our present work are in agreement with this description and provide a surprisingly easy method with which to determine the mass–length ratio of fibrin fibers in gels, provided the gels have a measurable opacity, i.e., are neither very dilute nor very "fine". (For gels with a low opacity, the mass–length ratio of the fibers can, of course, be obtained by measuring the light scattering, but this requires more specialized equipment.)

By analyzing the wavelength dependence of the turbidity, it is possible to make the important distinction between fiber formation and precipitation. Were it not for the possible contribution of a precipitate of fibrinogen or fibrin to the turbidity, optical densities at a single wavelength could be used to calculate fiber mass–length ratios.

The radius of fibers in fibrin gels had previously been estimated with electron microscopy of dried preparations. The radii obtained from turbidity measurements are those of wet fibers. Furthermore, these measurements give mass–length ratio, μ, and radius, r, of the same fibers and therefore permit calculation of fiber density, δ, with[16]

$$\mu = \pi\delta r^2$$

The fiber density calculated from our results (Figure 5) is 0.28. Since the protein has a density of approximately 1.39,[3] the volume of the fiber is 5.0 times the volume of the protein.

In the presence of only a small amount of thrombin, fiber growth is spread over a period of many hours, rather than over a few minutes. By lowering the thrombin concentration, the rate of fiber formation is reduced and fiber size increases. The ratio of fiber volume to protein volume is independent of the rate at which the fibers are formed; this suggests that the structure of the fibers is not variable and may be as highly ordered laterally as electron microscopy and x-ray diffraction show it to be longitudinally. Eventually, x-ray diffraction studies can determine the lateral order in fibers of large diameter. If these show that the fibrin fiber is crystalline, and a crystallographic unit cell is established, then the density which we have obtained may serve to calculate the number of fibrin molecules in the unit cell.

If each fibrin molecule takes up 450 Å in the fiber direction, as several studies suggest,[10,17–23] then the cross-sectional area of a molecule is calculated to be equal to that of a square with sides of 67 Å. It is probable that the interstices between fibrin molecules are filled with solvent, as in the case of protein crystals. The volume ratio is at the high end of the range observed for protein crystals. On the average, the ratio of crystal volume to protein volume is higher for proteins of high molecular weight, but even among the group of crystallized proteins with molecular weights over 10^5, there is only one example for which the volume ratio is as high as it is for the fibrin fiber, and on the average it is twice as small.[24] Recently

described crystals of a modified fibrinogen have a volume ratio of 2.9.[25]

We suggest that the solvent space inside the fibrin fiber has the form of channels through which protein molecules can diffuse. We think here in particular of two plasma enzymes, factor XIIIa and plasmin, which respectively stabilize fibrin by the introduction of covalent cross-links and cleave fibrin, destroying the fibrous structure. It does not appear that the action of these enzymes is impeded in fibers with a large diameter[4] and this may be taken as evidence that enzymes can penetrate inside the fibers. This requires that the fibers have the open structure for which we now have direct evidence.

The analogy between protein crystal and fibrin fiber should definitely not be extended to the intermolecular contacts holding these structures together. The intermolecular contacts in protein crystals are weak and nonspecific and usually these crystals form but slowly after a considerable adjustment of the solvent composition in order to drive the protein out of solution. The fibrin fiber is held together by high-affinity, specific contacts between monomers and the fibers form rapidly under physiological conditions. As a consequence of the fibers' low density, only a fraction of the surface of each monomer can be engaged in intermolecular contacts, the remainder being surrounded by solvent. This means that the contact sites should be thought of as discrete patches on the surface of the monomer.

IV. Theory

The turbidity, τ, of a solution is a measure of the intensity decrease of transmitted light due to scattering and can be calculated by integration of the scattered intensity over all possible directions. For solutions, the scattered intensity depends on the angle, θ, between the primary beam and the scattering direction. Hence,

$$\tau = \int_0^{\pi} 2\pi d^2(i_\theta/I_0) \sin\theta \, d\theta \tag{1}$$

$$i_\theta/I_0 = R_\theta(1 + \cos^2\theta)/d^2 \tag{2}$$

where i_θ is the scattered intensity per unit of volume, I_0 is the intensity of the primary beam, and d is the distance between scattering volume and detector. The scattering factor R_θ depends on the mass and dimensions of the particles. According to theory,[26–28] for very long and thin rodlike particles, the scattering factor is given by

$$R_\theta = cK\lambda\mu/4n \sin(\theta/2) \tag{3}$$

where c is the concentration, λ is the wavelength in vacuo, μ is the mass–length ratio of the fibers (in dalton/cm), and n is the refractive index of the solution. The constant K is given by

$$K = 2\pi^2 n^2 (dn/dc)^2/N\lambda^4 \tag{4}$$

where dn/dc is the specific refractive index increment of the solute in the solvent and N is Avogadro's number (throughout this paper, we make the assumption that the scattering does not deviate significantly from the Rayleigh-Debye limit).

It has been shown[9,28] that eq 2–4 give a good description of experimentally observed light scattering by fibrin fibers. Substituting eq 2 and 3 into eq 1 and integrating, one obtains[29]

$$\tau = (44/15)\pi Kc\lambda\mu/n \tag{5}$$

Since K, λ, and n are known parameters, one can in principle calculate the mass–length ratio of the fibers from the measured turbidity of a gel of known concentrations. Equation 5 also implies that the turbidity should vary as $1/\lambda^3$, if we neglect the slight wavelength dependence of n and of dn/dc.

The data presented show that the turbidity of fibrin gels is proportional to $1/\lambda^3$ over a considerable wavelength range but that the proportionality breaks down for gels with a very large mass–length ratio. This breakdown is presumably due to the fact that the diameter of fibers with a large mass–length ratio is not small compared with the wavelength. Whenever that is the case, the turbidity will not be as large as calculated with eq 5. The following relation can now be used:

$$(44/15)\pi Kc\lambda/n\tau = \mu^{-1}(1 + 184\pi^2\rho^2n^2/77\lambda^2 \ldots) \tag{6}$$

This result is obtained by integrating a similar expansion for the light-scattering intensity in powers of $\rho \sin(\theta/2)/\lambda$.[30,31] It follows that if one plots $c\lambda^3/\tau$ as a function of $1/\lambda^2$, then the intercept of the plot can be used to calculate the mass–length ratio, while the ratio of the initial slope and the intercept of the plot can be used to calculate the square of an average dimension, ρ (radius of gyration), which is determined by size and shape of the fibers' cross section. This kind of plot is analogous to the plot of Kc/R_θ vs. $\sin^2(\theta/2)$ commonly used to obtain molecular weight and radius of gyration from light scattering of molecularly dispersed particles.[32]

For *cylindrical* fibers of radius r, one may use the series expansion, eq 6, with

$$\rho^2 = r^2/2 \tag{7}$$

Alternatively, the scattering by cylindrical particles of very great length may be obtained by multiplying the expression for R_θ of eq 3 by a factor P_θ depending on the fiber radius and the scattering angle,

$$P_\theta = 4[J_1(x)/x]^2 \tag{8}$$

where

$$x = 4\pi r \sin(\theta/2)n/\lambda \tag{9}$$

and J_1 is the first-order Bessel function.[33,34] Integrating the scattered intensity to give the turbidity,

$$n\tau/\pi Kc\lambda = 16\mu\left[\upsilon^{-1}\int_0^{\upsilon} dx\, x^{-2}J_1^2(x) - 2\upsilon^{-3}\int_0^{\upsilon} dx\, J_1^2(x) + 2\upsilon^{-5}\int_0^{\upsilon} dx\, x^2J_1^2(x)\right] \tag{10}$$

where

$$\upsilon = 4\pi r/\lambda \tag{11}$$

We have evaluated the integrals numerically and from them calculated $1/\tau\lambda^3$ as a function of the ratio between cylinder radius and wavelength. We find that if one assumes that $1/\tau\lambda^3$ simply varies linearly with $1/\lambda^2$ and neglects higher order terms, then the calculated slope will not be seriously in error, as long as no observations are used for which $1/\tau\lambda^3$ is greater than twice its extrapolated value.

Finally, we give the values of the constants required in order to calculate the mass–length ratio and the square of the radius of fibrin fibers from intercept and initial slope of a plot of $c\lambda^3/\tau$ vs. $1/\lambda^2$ with eq 6 and 7 (Figure 4). These are, respectively,

$$(44/15)\pi K\lambda^4/n = (44/15)2\pi^3 n(dn/dc)^2/N = 1.48 \times 10^{-23} \tag{12}$$

and

$$184\pi^2n^2/2 \cdot 77 = 20.9 \tag{13}$$

where the values for n of water and dn/dc of fibrinogen at 633 nm have been used. Notice that the wavelength should be expressed in cm and the concentration in g/cm^3. The calculated mass–length ratio will be in dalton/cm and the radius in cm.

References and Notes

(1) This work was supported by a research grant from the National Institutes of Health (HL-20319).
(2) J. D. Ferry, *Adv. Protein Chem.*, **4**, 1 (1948).
(3) H. A. Scheraga and M. Laskowski, *Adv. Protein Chem.*, **12**, 1 (1957).
(4) R. Doolittle, *Adv. Protein Chem.*, **27**, 1–109 (1973).
(5) J. D. Ferry and P. R. Morrison, *J. Am. Chem. Soc.*, **69**, 388 (1947).
(6) S. Shulman and J. D. Ferry, *J. Phys. Colloid Chem.*, **54**, 66 (1950).
(7) D. F. Waugh and M. J. Patch, *J. Phys. Chem.*, **57**, 377 (1953).
(8) Z. S. Latallo, A. P. Fletcher, N. Alkjaersig, and S. Sherry, *Am. J. Physiol.*, **202**, 675 (1962).
(9) M. E. Carr, L. L. Shen, and J. Hermans, *Biopolymers*, **16**, 1 (1977).
(10) C. V. Z. Hawn and K. R. Porter, *J. Exp. Med.*, **86**, 285 (1947).
(11) N. V. Bang, *Thromb. Diath. Haemorr., Suppl.*, **13**, 73 (1964).
(12) D. Kay and B. J. Cuddigan, *Br. J. Haematol.*, **13**, 341 (1967).
(13) G. J. Stewart, *Scand. J. Haematol., Suppl.*, **13**, 165 (1970).
(14) J. M. Buchanan, L. B. Chen, T. Hamazaki, E. Lenk, and D. F. Waugh in "Chemistry and Biology of Thrombin", R. L. Lundblad, J. W. Fenton, and K. G. Mann, Ed., Ann Arbor Science Publication, 1977, p. 263.
(15) G. E. Perlman and L. G. Longsworth, *J. Am. Chem. Soc.*, **70**, 2719 (1948).
(16) Notice that the value of the mass–length ratio obtained by light scattering refers to the mass of the scattering material, i.e., the protein. The density calculated here is therefore very much different from the buoyant density of fiber plus solvent.
(17) K. R. Porter and C. V. Z. Hawn, *J. Exp. Med.*, **90**, 225 (1949).
(18) J. D. Ferry, S. Shulman, K. Gutfreund, and S. Katz, *J. Am. Chem. Soc.*, **74**, 5709 (1952).
(19) P. Kaesberg and S. Shulman, *J. Biol. Chem.*, **200**, 293 (1953).
(20) B. M. Siegel, J. P. Mernan, and H. A. Scheraga, *Biochim. Biophys. Acta*, **11**, 326 (1953).
(21) L. Stryer, C. Cohen, and R. Langridge, *Nature (London)*, **197**, 793 (1963).
(22) R. Gollwitzer, H. E. Karges, H. Hörmann, and K. Kühn, *Biochim. Biophys. Acta*, **207**, 445 (1970).
(23) W. Krakow, G. F. Endres, B. M. Siegel, and H. A. Scheraga, *J. Mol. Biol.*, **71**, 95 (1972).
(24) B. Mathews, *Annu. Rev. Phys. Chem.*, **27**, 493 (1976).
(25) N. M. Tooney and C. Cohen, *J. Mol. Biol.*, **110**, 363 (1977).
(26) T. Neugebauer, *Ann. Phys. (Leipzig)*, **42**, 509 (1943).
(27) A. Guinier and G. Fournet, "Small Angle Scattering of X-Rays", Wiley, New York, N.Y., 1955.
(28) E. F. Casassa, *J. Chem. Phys.*, **23**, 596 (1955).
(29) B. J. Berne, *J. Mol. Biol.*, **89**, 755 (1974).
(30) O. Kratky, *Makromol. Chem.*, **35a**, 12 (1960).
(31) V. Luzzati, *Acta Crystallogr.*, **13**, 939 (1960).
(32) B. H. Zimm, *J. Chem. Phys.*, **16**, 1099 (1948).
(33) R. G. Kirste, *Z. Phys. Chem. (Frankfurt am Main)*, **42**, 351 (1964).
(34) A. Fedorov and V. G. Aleshin, *Vysokomol. Soedin.*, **8**, 5016 (1966); *Polym. Sci. USSR (Engl. Transl.)*, **8**, 1657 (1967).

Nitric Acid Oxidation of High-Density Polyethylene. Organic Chemical Aspects

L. Russell Melby

Central Research and Development Department, E. I. du Pont de Nemours and Co., Wilmington, Delaware 19898.[1]

Received June 20, 1977

ABSTRACT: Preparative-scale nitric acid oxidation of bulk, high-density polyethylene has given high yields of nitrated α,ω-alkanedioic acids with molecular weights in the range 1300 to 3000 similar to products reported in the literature. The acids have polydispersity indexes of about 1.05–1.3 and thus are very nearly monodisperse. Carboxyl to nitro group ratios vary between about 6:1 and 1.6:1 depending on preparation conditions. Concentrated sulfuric acid converts the nitro groups to keto groups forming keto acids of unchanged molecular weight. Partial reduction of the keto groups can be achieved by the Clemmensen or Wolff–Kishner procedures. In some of the oxidation reactions, dinitroalkanedioic acids of molecular weight 400 to 500 were obtained; in these it is shown that the nitro groups are situated near the chain ends in positions α, β, or γ with respect to the carboxyl group.

The extensive work of Keller and his co-workers on the oxidation of polyethylene single crystals has done much to unravel the problem of fold surface structure in crystalline polyethylene.[2] In such oxidations, the amorphous chain folds at the periphery of the crystallites are severed and degraded back to the more resistant crystalline portions of the polymer.

Although some of the more recent work from Keller's laboratory used ozone as the oxidant,[3,4] most of the earlier work was done with fuming nitric acid[5,6] following similar previous studies by Palmer and Cobbold.[7] The products of the nitric acid oxidation were identified as nitrated, long-chain alkanoic acids,[6,8] and although some passing interest has been shown in chemical manipulation of such products as gel-permeation chromatography standards[9] or polymer intermediates,[10] most of the work in this area was done from a polymer physical structure viewpoint.

Thus, our attention was attracted to the organic chemistry of the process, its preparative aspects, and further characterization of the products.

Our characterization work in particular has clarified some inconsistencies in the literature and has led us to some further speculation on the course of the oxidation–nitration reaction.

Results and Discussion

Mechanics and Conditions of the Oxidation–Nitration Reaction. The nitric acid oxidations described in the literature were carried out on small amounts of carefully recrystallized polyethylene (0.1–0.3 g) in heated, sealed glass tubes and reaction times of 1 to 3 weeks.[5–10] Since our preparative work demanded large amounts of material, these limitations were unacceptable.

In preliminary experiments designed to permit larger scale development, several oxidations of high-density polyethylene pellets[11,12,13] were carried out on a 50-g scale in sealed rocker bombs. In general, these proceeded satisfactorily and gave products very similar to those of Keller et al. However, the potential explosion hazard of such systems, particularly if accidentally heated above the polymer melt temperature, encouraged us to explore the reaction in open vessels at atmospheric-pressure reflux temperatures. In this way, we were able to operate on a 200-g scale.

In most of the published work referred to, 95% fuming nitric acid was used although some was done with 82.5% acid.[4,8] Constant reaction temperatures of 60 or 80 °C were used. We worked with three different strengths of acid, namely, ordinary concentrated (71% HNO_3), 90% fuming, and red fuming

0024-9297/78/2211-0050$01.00/0